Performance Assessment of a Generic Nuclear Waste Repository in Shale – 18392

Emily Stein *, Paul Mariner *, Jennifer Frederick *, David Sevougian *, Glenn Hammond *
* Sandia National Laboratories

ABSTRACT

A performance assessment (PA) is an important component of a comprehensive safety analysis for a nuclear waste repository. In a PA, probabilistic simulations of the total repository system are performed, and results are evaluated against performance metrics. Uncertainty and sensitivity analyses help prioritize additional research and model development. The United States Department of Energy (DOE) has been developing a state of the art PA simulation software toolkit, Geologic Disposal Safety Assessment (GDSA) Framework, that couples increasingly higher fidelity models of subsystem processes into total system PA simulations. Over the past several years, PAs of generic repositories in three geologic media (salt, shale, and crystalline rock) have demonstrated ongoing developments in capability. The current PA of a nuclear waste repository in a generic shale formation showcases GDSA Framework, including capabilities in domain discretization (Cubit), multiphysics simulations (PFLOTRAN), uncertainty and sensitivity analysis (Dakota), and visualization (Paraview).

The generic shale reference case considers the disposal of 22,000 metric tons heavy metal of commercial spent nuclear fuel (SNF) in a generic shale formation. PA simulations account for the thermal load and radionuclide inventory of the waste form, components of the engineered barrier system including waste package and buffer, and components of the natural barrier system including the host rock shale and underlying and overlying stratigraphic units. Two repository layouts are considered, one for emplacement of waste packages containing 12 pressurized water reactor (PWR) assemblies, and one for 4-PWR waste package emplacement. Model domains are half-symmetry and contain between 7 and 22 million grid cells. Grid refinement captures the detail of individual waste packages, emplacement drifts, access drifts, and shafts. Simulations are run in a high-performance computing (HPC) environment on 512 or 2048 processes. The governing equations describing coupled heat and fluid flow and reactive transport are solved with PFLOTRAN, an open-source, massively parallel multiphase flow and reactive transport code. Additional simulated processes include waste package degradation; waste form dissolution; radioactive decay and ingrowth in aqueous, solid, and adsorbed phases; and a simple biosphere based on a pumping well. Simulations are run to 10^6 y; dose and radionuclide concentrations are observed within aquifers at a point approximately 5 km downgradient of the repository. Dakota is used to sample likely ranges of input parameters including waste form and waste package degradation rates and properties of engineered and natural materials to quantify uncertainty in predicted concentrations and sensitivity to input parameters.

Given the assumptions of the reference case, results of 12-PWR and 4-PWR simulations are very similar. Dose at the pumping well 5-km downgradient of the repository does not exceed 10^{-9} Sv/y. I-129 is the largest contributor to dose. The dose due to Cl-36, the next largest contributor, is orders of magnitude smaller. At the pumping well, the concentration of I-129 5-km downgradient does not exceed 10^{-14} mol/L. Rank correlation coefficients indicate that the maximum concentration of I-129 within the aquifer is sensitive to shale (repository host rock) porosity and aquifer permeability. These results affirm that HPC-capable codes can be used to simulate important multi-physics couplings directly in a total system performance assessment of a geologic repository, and can be used in prioritization of future research and model development.

INTRODUCTION

A computational framework for repository performance assessment must keep up with continued advances in computational capabilities and with continued development of physics and chemistry (process) models. The long-term vision for GDSA Framework [1] is to ensure that it can adapt to, and take advantage of, future advances in computational software and hardware and future advances in process modeling. The

near-term mission is to integrate new process models important to repository performance and to develop a robust suite of fully functional repository reference case applications. These efforts will provide a basis for evaluating the sensitivity of model results to features, processes, and parameters, which can be used to prioritize future disposal R&D.

In this paper, we describe GDSA Framework and demonstrate its capability in application to a shale repository reference case.

GDSA FRAMEWORK

Overview

A probabilistic PA requires a large number of simulations of a complex system. For this reason, GDSA Framework is designed for massively-parallel processing. Two open-source, HPC codes are the core of GDSA Framework: PFLOTRAN and Dakota. PFLOTRAN [2] is a massively-parallel multiphase flow and reactive transport code, and Dakota [3] is a versatile probabilistic code. Other components of GDSA Framework include an input parameter database, and support software and scripts for meshing (Cubit [4]), pre- and post-processing (Python), and visualization (Paraview [5]). Integration of new process models and capabilities is accomplished through development of PFLOTRAN and through coupling of external codes, such as Fuel Matrix Degradation Model (FMDM) [6].

The flow of data and calculations through these components is illustrated in Fig. 1. In a probabilistic simulation, Dakota generates stochastic input for each PA realization based on parameter uncertainty distributions defined in the input set. The sampled inputs are used by PFLOTRAN and its coupled process models to simulate the radionuclide source term, evolution of the engineered barrier system (EBS), flow and transport through the EBS and the natural barrier system (NBS), and uptake in the biosphere. After the simulation, various software packages may be used to reduce and illustrate simulation output. Dakota may also be used to evaluate the effects of parameter uncertainty on specific outputs.

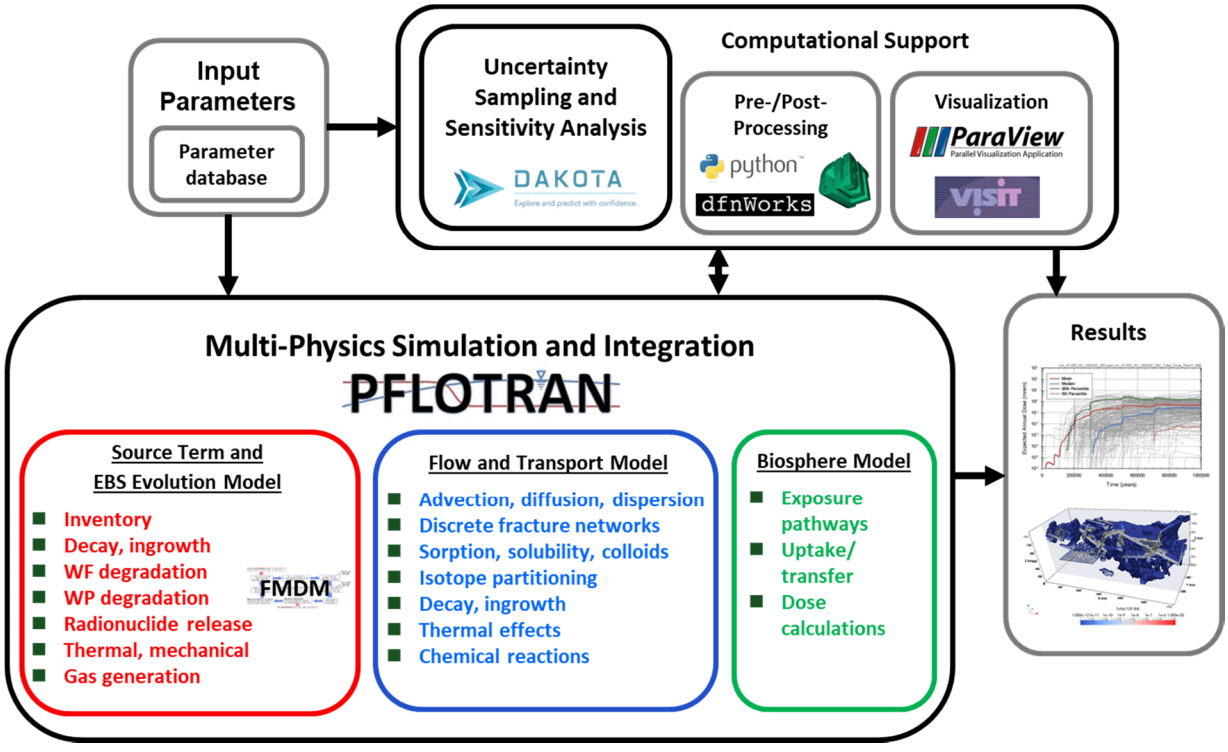

Fig. 1. GDSA Framework structure.

Repository-Specific Process Models

The isotope partitioning process model [7,8] simulates radionuclide decay and ingrowth in all phases by partitioning isotopes among aqueous, adsorbed, and precipitate phases on the basis of element-specific adsorption coefficients (e.g., K_d values) and element-specific solubility limits. The isotope partitioning model maximizes entropy, i.e., distributes isotopes of the same element across the phases such that the isotope mole fractions for a given element are the same in each phase.

The waste form process model [7,8] is used to calculate the radionuclide source term for each waste package in the model domain. It simulates waste package degradation, waste form dissolution, and radionuclide decay and ingrowth within the waste form. At this time, waste package degradation is modeled as temperature-dependent general corrosion. The waste package degradation rate (normalized to the thickness of the waste package wall) (R_{eff}) is calculated according to

$$R_{eff} = R \cdot e^{C\left(\frac{1}{333.15} - \frac{1}{T(t,\vec{x})}\right)} \quad \text{(Eqn. 1)}$$

where R is the base normalized waste package degradation rate at 60ºC, T is the local temperature (in Kelvin), and C is the canister material constant. The base degradation rate, R, can be sampled from a truncated log normal distribution, creating heterogeneity in waste package degradation rates. When waste package wall thickness reaches zero, the waste package is breached, and waste form dissolution begins. Mechanisms available for waste form dissolution include instantaneous dissolution (for, e.g., metallic waste forms), glass dissolution, oxidative dissolution via the Fuel Matrix Degradation Model [6], and a fractional degradation rate, which may be applied to either the remaining or initial volume of waste. An instant release fraction for each radionuclide in the waste form may also be specified. For these simulations of commercial (UO_2) SNF, we specified instant release fractions and a fractional degradation rate applied to remaining waste volume.

The biosphere process model [8] calculates the ingestion dose rate for a person regularly consuming contaminated well water. It includes dose due to short-lived daughter products not explicitly modeled in transport calculations by assuming secular equilibrium with parents, and accounts for the distribution of parents and daughters between aqueous and adsorbed phases.

SHALE REPOSITORY REFERENCE CASE

Geologic Setting

Clay-rich sedimentary strata have been considered a potential medium for disposal of radioactive waste in the United States since the forerunner to the DOE introduced a program to develop radioactive waste disposal technology in 1976, e.g. [9]. Clay-rich formations are an attractive disposal medium due to their low permeability, high sorption capacity, typically reducing pore water (which limits radionuclide solubility), and ability to deform plastically, which promotes self-healing of fractures. The U.S. hosts several marine sedimentary sequences containing thick beds of clay-rich sediments potentially suitable for deep geologic disposal of radioactive waste [10]. Locations of aerially extensive shale formations in the U.S. are shown in Fig. 2.

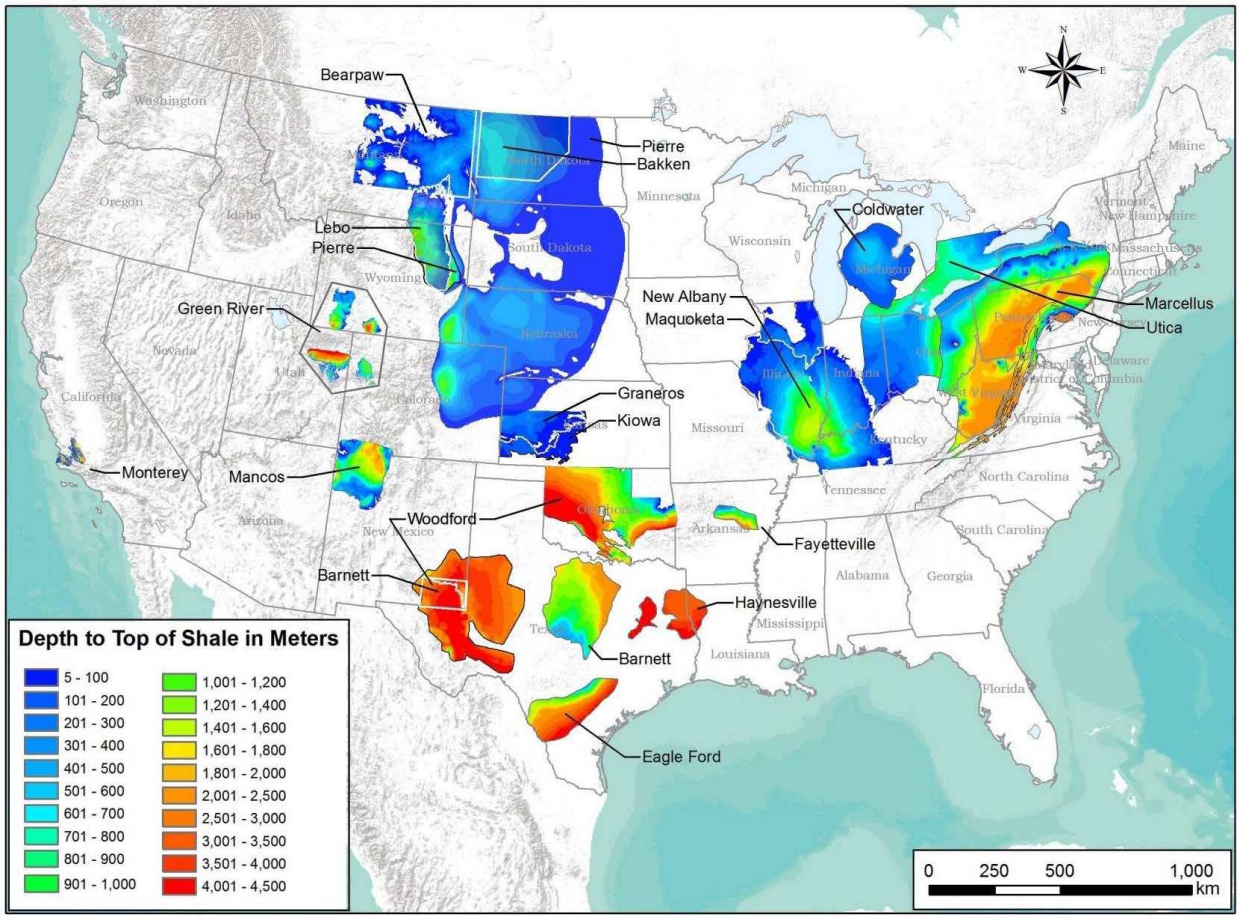

Fig. 2. Locations of areally extensive shale formations in the U.S. [10].

Engineered Barrier Characteristics

The shale reference case assumes a mined repository located approximately 500 m below land surface, accessed by vertical shafts, and containing 70,000 MTHM of commercial SNF, which is the maximum allowed by the Nuclear Waste Policy Act of 1983 and about half of the total commercial SNF inventory predicted by 2055 in the "no replacement scenario" [11].

This inventory could be accommodated in 13,398 12-PWR waste packages in 268 1035-m long emplacement drifts, each containing 50 waste packages emplaced lengthwise and spaced 20 m center-to-center. A 25-m long seal is placed at either end of each emplacement drift. Drifts are 4.5 m in diameter spaced 30 m center-to-center. These dimensions would result in a total emplacement footprint of approximately 8.3 km^2.

Alternatively, the 70,000-MTHM inventory could be accommodated in 40,194 4-PWR waste packages in 4466 100-m long horizontal emplacement boreholes, each containing 9 waste packages spaced 10 m center-to-center. Thirty-five boreholes are spaced 30 m apart (center-to-center) along each side of 64 access drifts, 1035 m in length and 5.5 m in diameter. Access drifts are spaced 235-m center-to-center, leaving a 30-m distance between the ends of aligned boreholes. These dimensions would result in a total emplacement footprint of approximately 15.6 km^2.

PA simulations use a half-symmetry model domain, in which approximately 15% (10,962 MTHM) of the 70,000 MTHM inventory is explicitly gridded. With the reflection boundary condition, 30% (21,924 MTHM) of the 70,000 MTHM inventory is included.

For simplicity, PA simulations assume that the inventory consists entirely of PWR SNF assemblies, each containing 0.435 MTHM. Radionuclide inventories and decay heat versus time curves are taken from Carter et al. [11] and assume an initial enrichment of 4.73 wt% U-235, 60 GWd/MTHM burn-up, and 100-year out of the reactor (OoR) storage prior to deep geologic disposal. Because the average burn-up of SNF under the "no replacement scenario" is predicted to be only 54 GWd/MTHM [11], the assumption of 60 GWd/MTHM results in a conservatively high heat load. Inventories of the 18 radionuclides included in PA simulations are given in Table 1.

Table I. Radionuclide inventories and element solubilities and adsorption coefficients [8].

Element	Isotope	Inventory (g/MTIHM)	Solubility (mol/L)	Shale K_d (mL/g)	Buffer K_d (mL/g)	Aquifer K_d (mL/g)
Am	Am-241	1.46E+03	4×10^{-7}	50,000	12,000	89.4
	Am-243	2.69E+02				
Pu	Pu-238	2.84E+02	2×10^{-7}	900	1000	447
	Pu-239	7.40E+03				
	Pu-240	4.11E+03				
	Pu-242	8.17E+02				
Np	Np-237	1.40E+03	4×10^{-9}	900	1000	14.1
U	U-233	4.33E-02	7×10^{-7}	8000	100,000	0.775
	U-234	5.11E+02				
	U-236	6.27E+03				
	U-238	9.10E+05				
Th	Th-229	1.48E-05	6×10^{-7}	8000	3000	2646
	Th-230	1.04E-01				
Ra	Ra-226	3.99E-05	1×10^{-7}	1000	1000[e]	Non-adsorbing
Cl	Cl-36	5.01E-01	Infinite	Non-adsorbing	Non-adsorbing	Non-adsorbing
Tc	Tc-99	1.28E+03	4×10^{-9}	1150	114,000	50
I	I-129	3.13E+02	Infinite	Non-adsorbing	Non-adsorbing	Non-adsorbing
Cs	Cs-135	7.72E+02	Infinite	400	380	500

The reference EBS also includes waste packages that consist of a stainless steel canister with a stainless steel overpack, and a bentonite/sand buffer/backfill in access and emplacement drifts, emplacement boreholes, and shafts. Material properties used in deterministic simulations are listed in Table 2. Although other materials would likely be present in a shale repository (e.g. cement liners, seals of compacted bentonite, or crushed rock backfill), these materials are not modeled in PA simulations.

Table II. Material properties used in deterministic simulations [8].

Model Region	Permeability (m^2)	Porosity ϕ	τ	Effective Diffusion Coefficient (m^2/s)	Saturated Thermal Conductivity (W/m/K)	Heat Capacity (J/kg/K)	Grain Density (kg/m^3)
Overburden	1×10^{15}	0.20	0.11	2.2×10^{11}	1.7	830	2700
Upper Sandstone	1×10^{-13}	0.20	0.58	1.2×10^{10}	3.1	830	2700
Host Rock Shale	1×10^{-19}	0.20	0.11	2.2×10^{11}	1.2	830	2700
Silty Shale	1×10^{-17}	0.20	0.11	2.2×10^{11}	1.4	830	2700
Limestone	1×10^{14}	0.10	0.04	4.0×10^{12}	2.6	830	2700
Lower Shale	1×10^{20}	0.10	0.04	4.0×10^{12}	1.2	830	2700
Lower Sandstone	1×10^{-13}	0.20	0.58	1.2×10^{10}	3.1	830	2700
Buffer	1×10^{20}	0.35	0.23	8.1×10^{11}	1.5	830	2700
Waste Package	1×10^{16}	0.50	1	5×10^{10}	16.7	466	5000

Natural Barrier Characteristics

The natural barrier system (NBS) comprises the shale formation hosting the repository, the disturbed rock zone (DRZ) adjacent to the repository, and geological formations above and below the host formation. The reference case assumes a stratigraphic column consisting of (from the bottom up): a 450 m thickness of indurated shale interrupted by a 30-m thick sandstone aquifer; a 75-m thick limestone aquifer; a 585 m thickness of sealing shale (the host rock) including a 90 m thickness of a silty shale unit; a 60-m thick sandstone aquifer; and a 30 m thickness of unconsolidated overburden (Fig. 3) [10]. Material properties used in deterministic simulations are listed in Table 2.

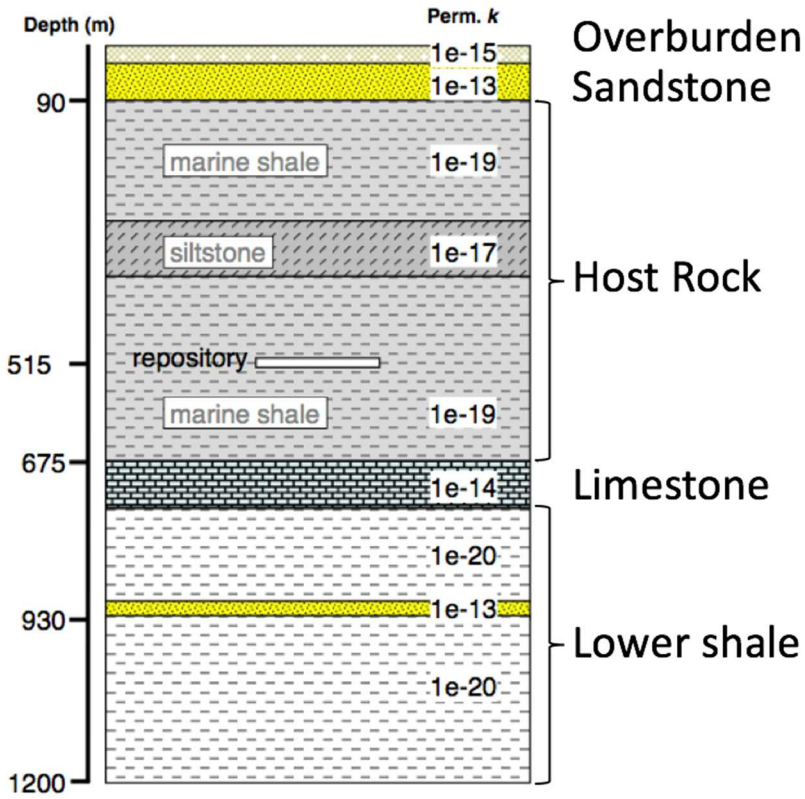

Fig. 3. Reference stratigraphic column [10].

Chemical Environment

Pore water of a deep, hydraulically isolated shale can be conceptualized as seawater (connate water) equilibrated (or partially so) with the surrounding mineral assemblage, isolated from the atmosphere, and in diffusive communication with pore waters of overlying and underlying geologic units, including aquifers in which water is flowing. Pore water composition within the shale will be transient on long time scales and dependent on distance to adjacent aquifers, pore water composition in adjacent aquifers, and time elapsed since the shale/aquifer system originated [12]. Overall, pore water is likely to be of moderate ionic strength, reducing, and of neutral to slightly alkaline pH. Assumed element solubilities and linear sorption coefficients (K_ds) for these conditions are given in Table 1.

Biosphere

The simple biosphere model includes a well pumping at a rate of 500 gallons per day (a rate that would supply drinking water for a rural family), located in the upper sandstone aquifer at a distance of 5 km down-gradient from the repository. The well's screened interval spans the 60-m thickness of the aquifer. The dose rate is calculated for an adult who consumes 2 liters per day on average, using ingestion dose coefficients from [13].

POST-CLOSURE PERFORMANCE ASSESSMENT

PA simulations, including one deterministic simulation each of the 12-PWR and 4-PWR cases and a suite of 50 probabilistic simulations for the 12-PWR case, assume (1) a mined repository at 515 m depth; (2) a head gradient of -0.0013 m/m from west to east; (3) a regional heat flux of 60 mW/m^2 and a mean annual surface temperature of 10 °C; and (4) a saturated model domain.

Simulated processes include waste package degradation, waste form (UO_2) dissolution, equilibrium-controlled radionuclide sorption and precipitation/dissolution, radioactive decay and ingrowth

in all phases (aqueous, adsorbed, precipitate), coupled heat and fluid flow, and radionuclide transport via advection and diffusion. Mechanical dispersion is conservatively neglected. Including it would result in earlier arrival of radionuclides at the well (and other observation points), but lower peak concentrations than reported here.

Model Domain and Discretization

Two model domains were gridded, one for 12-PWR simulations (Fig. 4) and one for the 4-PWR simulation (not shown). The half-symmetry model domains are 1575 m in width (*Y*) and 1200 m in height (*Z*). Each domain is long enough to place an observation point 5000 m down-gradient of the repository, making the 12-PWR domain 6855 m in length (*X*), and the 4-PWR domain (which has a longer repository footprint) 7935 m in length. Most of each domain is discretized into cells 15 m on a side. Emplacement drifts within the 12-PWR domain are discretized into cells 1.67 m (5/3 m) on a side. Emplacement boreholes within the 4-PWR domain are discretized into cells 0.56 m (5/9 m) on a side. Transitional zones of cells 5/3 m (in the 4-PWR domain) and 5 m (in both domains) on a side exist between the finely discretized emplacement zones and the remainder of the domain. The 12-PWR domain contains 6,925,936 cells, of which approximately 3 million are the smaller cells in and around the repository; simulations run on 512 processes each took less than 2 hours to complete. The 4-PWR domain contains 22,831,632 cells, of which approximately 18 million are the smaller cells in and around the repository; a simulation run on 2048 processes took approximately 5.5 hours to complete.

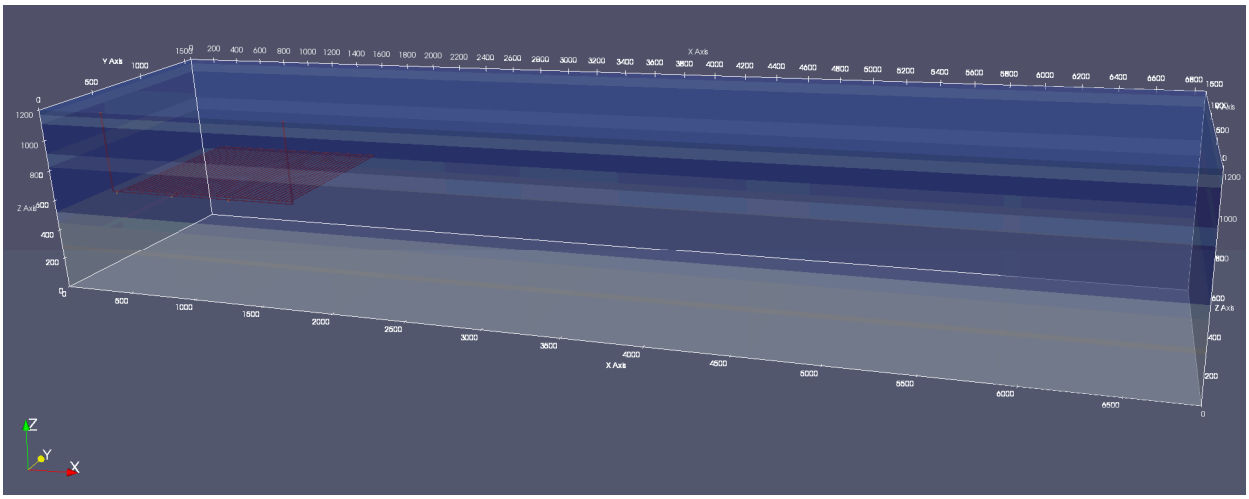

Fig. 4. Transparent view of the 12-PWR model domain colored by material. The repository is in red. Shades of blue represent the stratigraphic column shown in Fig. 3.

Initial and Boundary Conditions

Initial conditions specified are pressure, temperature, and radionuclide concentrations. Initial pressures and temperatures throughout the model domain are calculated by applying a liquid flux of 0 m/s and an energy flux of 60 mW/m^2 to the base of the domain and holding temperature (10°C) and pressure (approximately atmospheric) constant at the top of the domain, and allowing the simulation to run to 10^6 years. Pressure at the top of the domain decreases from west (left) to east (right) with a head gradient of -0.0013 (m/m). This technique results in initial conditions that represent a geothermal temperature gradient and hydrostatic pressure gradient in the vertical direction, and a horizontal pressure gradient that drives flow from west to east. Initial concentrations of all radionuclides in all cells are 10^{-20} mol/L.

Boundary conditions must be set for the six faces of the model domain. Fluxes of heat, fluid, and solute are set to zero at the south face of the model domain, creating a reflection boundary and virtually doubling the volume of the model domain. At all other faces, initial pressures and temperatures are held constant.

Radionuclide concentrations are held such that any fluid entering the model domain contains 10^{-20} mol/L of each radionuclide, while fluid exiting the model domain is allowed to carry with it ambient concentrations. Diffusive flux across outflow boundaries is disallowed by specifying a zero concentration gradient.

Waste Package Source Terms

Each waste package is modeled as a transient heat source. The energy (watts per waste package) entering the model domain is updated periodically according to values in a lookup table. The initial value is that for PWR SNF 100 yr OoR. For 12-PWR waste packages (5.22 MTHM), the initial value is 3084 W; for 4-PWR waste packages (1.74 MTHM), the initial value is 1028 W. Between times specified in the lookup table, the energy input is linearly interpolated.

The waste package degradation model (see above) calculates normalized remaining canister thickness at each time step as a function of a base canister degradation rate, a canister material constant, and temperature. Waste package breach occurs when this thickness reaches zero. Deterministic simulations assign a base canister degradation rate for each waste package by sampling on a truncated log normal distribution with a mean of $10^{-4.5}$/yr, a standard deviation of 0.5 (log units) and an upper truncation of -3.5 (log units).

From the time of waste package breach, the waste form releases radionuclides in two fractions: instant-release and slow-release. The instant-release fraction is due to the accumulation of fission products in void spaces of the waste form and occurs at the time of waste package breach. The shale reference case assumes a non-zero instant-release fraction for Cs-135, I-129, Tc-99, and Cl-36, and zero for all other radionuclides in the simulations. The slow-release fraction is due to fuel matrix (UO_2) dissolution, which is modeled using a fractional dissolution rate (applied to the remaining volume of waste) of 10^{-7}/yr starting from the time of waste package breach.

Deterministic Results

The difference between the 12-PWR case and the 4-PWR case is most apparent in predicted repository temperatures. In both cases, the background geothermal gradient results in an initial repository temperature of 27.8 °C. Waste package temperatures peak at approximately 20 years, reaching a high of 151 °C in the 12-PWR simulation and 104 °C in the 4-PWR simulation, and remain elevated above background for approximately 100,000 y. Because of the cooler temperatures in the 4-PWR repository, waste package breach times are slightly later than in the 12-PWR repository, with 50% of waste packages breached by 31,000 y in the 12-PWR case and by 41,000 y in the 4-PWR case. In both cases 99% of waste packages have breached by the end of the 1-million-year simulation.

The 12-PWR and 4-PWR simulations result in nearly identical concentrations at points within the upper sandstone aquifer (the conceptual path to the biosphere). For this reason, only 12-PWR results are discussed in more detail.

12-PWR results show that transport away from the repository is diffusive within the host rock, and begins when the earliest waste packages breach (Fig. 5). At 1000 y, a handful of waste packages have breached, and I-129 is confined to the immediate vicinity of the breached waste packages. At 10,000 y, fewer than 50% of the waste packages have breached, and I-129 remains confined to the near field. By 100,000 y, I-129 has reached the limestone aquifer, 160 m beneath the repository, at 10^{-15} M concentrations. By 1,000,000 y, I-129 has reached the upper sandstone aquifer, 425 m above the repository, at 10^{-15} M concentrations, and advected in both aquifers to the downstream end of the model domain, just over 5 km beyond the edge of the repository. Soluble, non-sorbing Cl-36 (not shown) behaves similarly to I-129, though concentrations are lower. Radionuclides that sorb and/or precipitate (e.g., isotopes of Am, Np, U, Th, etc.) remain in the vicinity of the repository throughout the 1-million-year simulation.

Dose at the pumping well located 5-km downgradient in the upper aquifer is entirely due to I-129 and Cl-36. Dose rate reaches a maximum of less than 2 x 10^{-10} Sv/yr at 1,000,000 y (orange line in Fig. 6d). For comparison, the international safety standard recommended by the IAEA for the public is 10^{-3} Sv/yr [14].

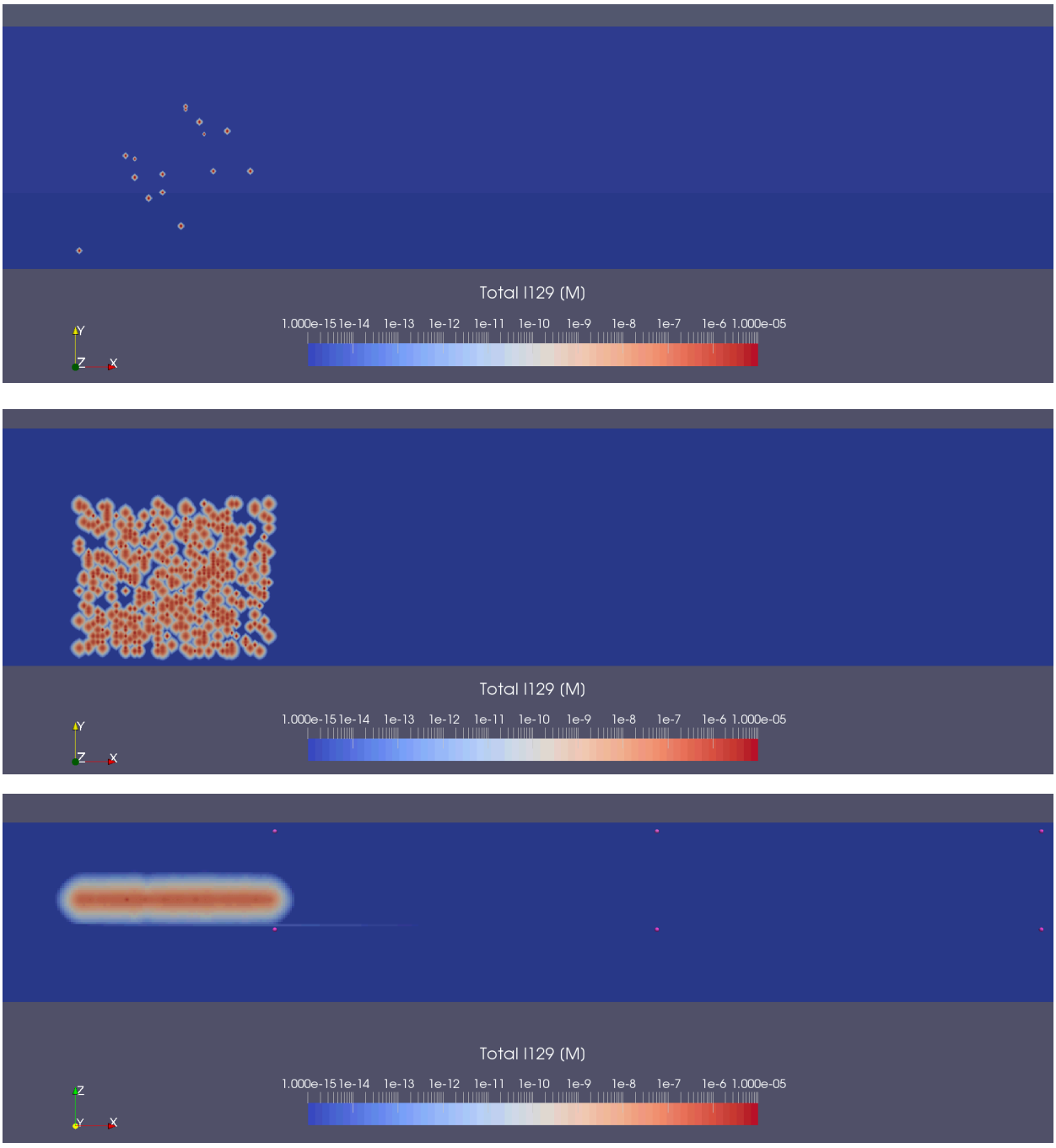

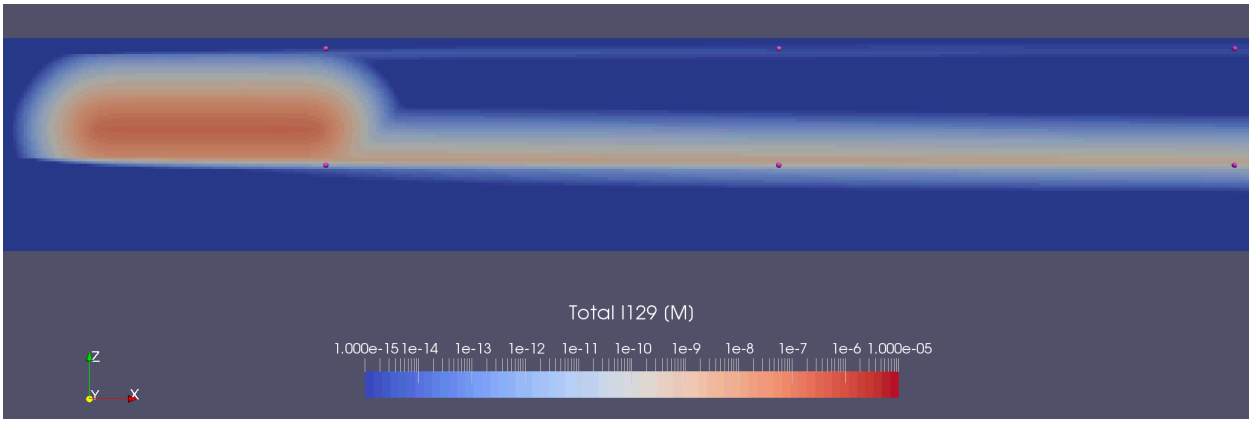

Fig. 5. I-129 concentration in the deterministic 12-PWR simulation at (from top to bottom) 1000 y (horizontal slice); 10,000 y (horizontal slice); 100,000 y (vertical slice); 1,000,000 y (vertical slice). Pink dots indicate location of observation points discussed in Probabilistic Results section.

PROBABILISTIC RESULTS

A suite of 50 probabilistic simulations was run using the 12-PWR model domain and the parameter distributions listed in Table 3. Concentrations of I-129 at three observation points in the upper sandstone aquifer and three observation points in the limestone aquifer (discussed in [8]) were used to quantify uncertainty and sensitivity. In each aquifer, observation points (pink dots in Fig. 5) are approximately 30, 2500, and 5000 m downgradient of the repository.

Table III. Parameter distributions used in probabilistic simulations [8].

Parameter	Range	Units	Distribution
SNF Dissolution Rate	10^{-8} – 10^{-6}	yr^{-1}	log uniform
Mean Waste Package Degradation Rate	$10^{-5.5}$ – $10^{-4.5}$	yr^{-1}	log uniform
Upper Sandstone k	10^{-15} – 10^{-13}	m^2	log uniform
Limestone k	10^{-17} – 10^{-14}	m^2	log uniform
Lower Sandstone k	10^{-14} – 10^{-12}	m^2	log uniform
Buffer k	10^{-20} – 10^{-16}	m^2	log uniform
DRZ k	10^{-18} – 10^{-16}	m^2	log uniform
Host Rock (Shale) Porosity	0.1 – 0.25	-	uniform
Np K_d Buffer	0.1 – 702	m^3kg^{-1}	log uniform
Np K_d Shale	0.047 – 20	m^3kg^{-1}	log uniform

Uncertainty

Breakthrough curves for I-129 in the upper sandstone aquifer and dose at the pumping well are plotted in Fig. 6. In all simulations, I-129 concentration remains less than 10^{-12} M at "sand_obs1," less than 10^{-13} M at "sand_obs2," and less than 10^{-15} M at "sand_obs3," 5000 m downgradient of the repository. At all three locations, maximum predicted I-129 concentration varies by 6 to 7 orders of magnitude. Dose rate at the pumping well does not exceed 10^{-9} Sv/yr, and in approximately 40% of the simulations does not exceed the dose rate due to initial radionuclide concentrations.

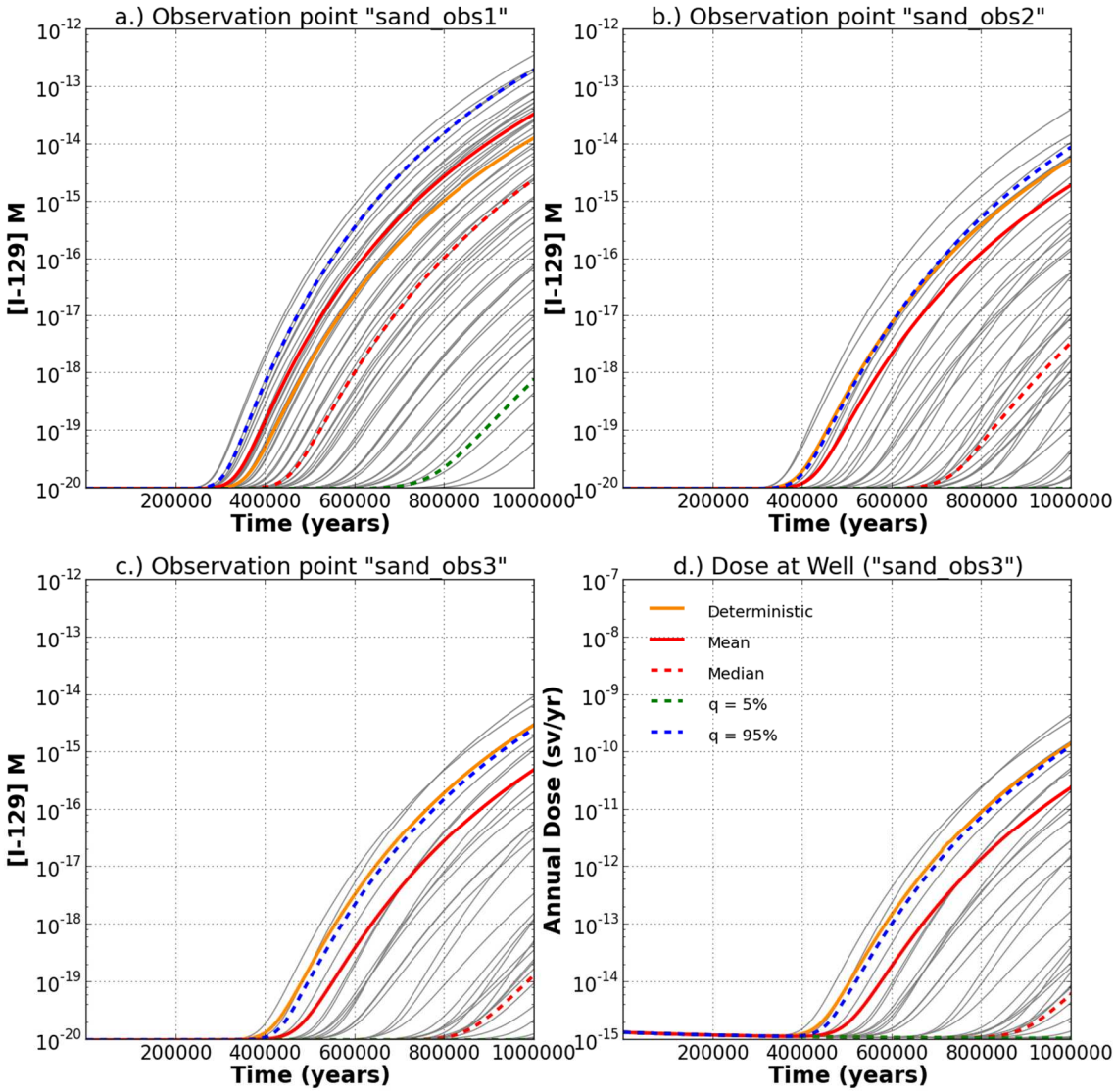

Fig. 6. I-129 concentration in the upper sandstone aquifer approximately 30 m (a), 2500 m (b), and 5000 m (c) downgradient of the repository; and dose at the pumping well (d), the location of which coincides with observation point "sand_obs3".

Sensitivity

Spearman rank correlation coefficients were calculated using Dakota to assess the sensitivity of maximum concentration of I-129 to sampled parameters (Fig. 7). Maximum concentration of I-129 in the upper sandstone aquifer exhibits a strong positive correlation with shale porosity ("Shale ϕ") and a weak

negative correlation with aquifer permeability ("U. Sand *k*") at "sand_obs1." Sensitivity to shale porosity decreases with distance from the repository, while the correlation with aquifer permeability becomes positive and increases in strength.

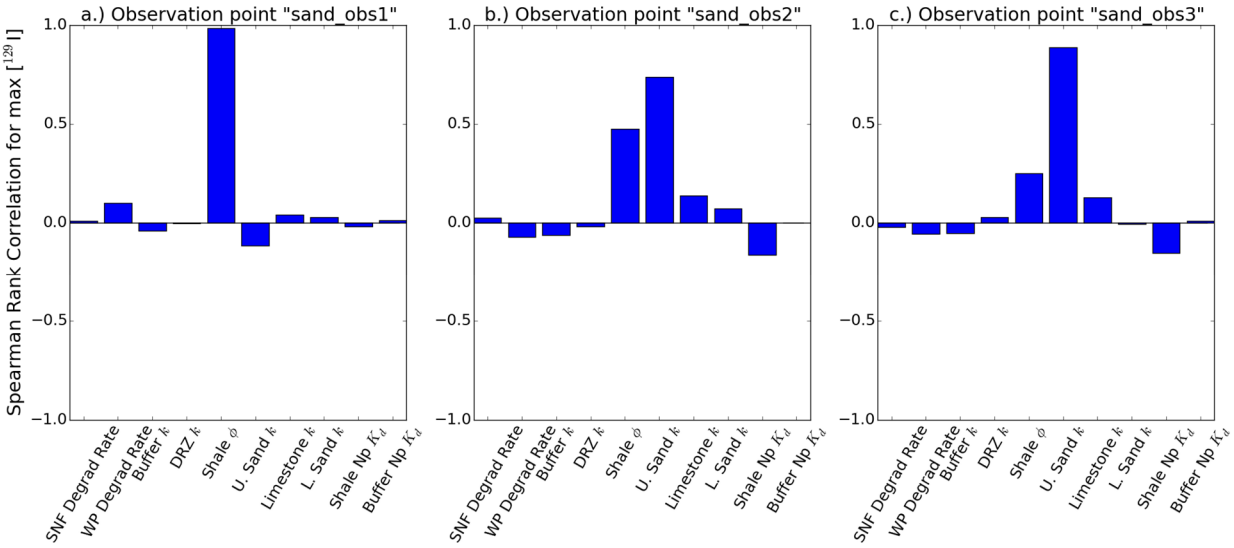

Fig. 7. Spearman rank correlation coefficients relating maximum I-129 concentration in the upper sandstone aquifer to sampled input parameters.

CONCLUSIONS

GDSA Framework is a software toolkit for modeling geologic disposal of nuclear waste that can be used to probabilistically assess the performance of disposal options and proposed sites. It employs HPC-capable codes PFLOTRAN and Dakota, as well as Cubit, Paraview, and Python for pre- and post-processing. Development of coupled process models such as isotope partitioning, decay, and ingrowth; waste package and waste form degradation; and the ingestion dose model enables simulation of multi-physics processes within a total system performance assessment. Future integration of coupled process models will expand this capability.

Simulation of increasingly complicated problems continues to affirm that HPC-capable codes can be used to simulate important multi-physics couplings directly in a total system performance assessment of a geologic repository. Repository reference cases modeled to date, including the 12-PWR and 4-PWR shale cases presented here, indicate that GDSA Framework can simulate complex coupled processes in a multi-kilometer domain while simultaneously simulating sub-meter-scale coupled behavior in the repository. Simulations like these can provide a basis for evaluating the sensitivity of model results to features, processes, and parameters, and can be used to prioritize future repository research and model development.

REFERENCES

1. SNL (2017). "GDSA Framework: A Geologic Disposal Safety Assessment Modeling Capability," pa.sandia.gov.

2. Hammond, G. E., P. C. Lichtner, C. Lu and R. T. Mills (2011a). "PFLOTRAN: Reactive Flow and Transport Code for Use on Laptops to Leadership-Class Supercomputers." Groundwater Reactive Transport Models. F. Zhang, G. T. Yeh and J. Parker. Bentham Science Publishers.

3. Adams, B. M., K. R. Dalbey, M. S. Eldred, L. P. Swiler, W. J. Bohnhoff, J. P. Eddy, D. M. Vigil, P. D. Hough and S. Lefantzi (2012). DAKOTA, A Multilevel Parallel Object-Oriented Framework for Design

Optimization, Parameter Estimation, Uncertainty Quantification, and Sensitivity Analysis: Version 5.2+ User's Manual. SAND2010-2183. Sandia National Laboratories, Albuquerque, New Mexico.

4. Blacker, T., S. J. Owen, M. L. Staten, R. W. Quador, B. Hanks, B. Clark, R. J. Meyers, C. Ernst, K. Merkley, R. Morris, C. McBride, C. Stimpson, M. Plooster and S. Showman (2016). CUBIT Geometry and Mesh Generation Toolkit 15.2 User Documentation. SAND2016-1649 R. Sandia National Laboratories, Albuquerque, New Mexico.

5. Ahrens, J., Geveci, B., Law, C. (2005). *Paraview: An End-User Tool for Large Data Visualization*, Visualization Handbook, Elsevier, ISBN-13: 978-0123875822.

6. Jerden, J., G. Hammond, J. M. Copple, T. Cruse and W. Ebert (2015). Fuel Matrix Degradation Model: Integration with Performance Assessment and Canister Corrosion Model Development. FCRD-UFD-2015-000550. US Department of Energy, Washington, DC.

7. Mariner, P. E., E. R. Stein, J. M. Frederick, S. D. Sevougian and G. E. Hammond (2016). Advances in Geologic Disposal System Modeling and Application to Crystalline Rock. FCRD-UFD-2016-000440, SAND2016-9610 R. Sandia National Laboratories, Albuquerque, New Mexico.

8. Mariner, P. E., E. R. Stein, J. M. Frederick, S. D. Sevougian and G. E. Hammond (2017). Advances in Geologic Disposal System Modeling and Shale Reference Cases. FCRD-UFD-2017-000044, SAND2017-10304 R. Sandia National Laboratories, Albuquerque, New Mexico.

9. Shurr, G. W. (1977). The Pierre Shale, Northern Great Plains: A Potential Isolation Medium for Radioactive Waste. Open-File Report. United States Geological Survey. Reston, VA**:** 27.

10. Perry, F. V. and R. E. Kelley (2017). Regional Geologic Evaluations for Disposal of HLW and SNF: The Pierre Shale of the Northern Great Plains. Los Alamos National Laboratory. Los Alamos, NM.

11. Carter, J. T., A. J. Luptak, J. Gastelum, C. Stockman and A. Miller (2013). Fuel Cycle Potential Waste Inventory for Disposition. FCRD-USED-2010-000031 Rev 6. Savannah River National Laboratory, Aiken, South Carolina.

12. Mazurek, M., P. Alt-Epping, A. Bath, T. Gimmi, H. N. Waber, S. Buschaert, P. De Canniere, M. De Craen, A. Gautschi, S. Savoye, A. Vinsot, I. Wemaere and L. Wouters (2011). "Natural tracer profiles across argillaceous formations," *Applied Geochemistry*, **26**(7):1035-1064.

13. ICRP (2012). Compendium of Dose Coefficients based on ICRP Publication 60. ICRP Publication 119. Ann. ICRP 41(Suppl.). Elsevier Ltd. for the International Commission on Radiological Protection (ICRP)

14. IAEA (2014). Radiation protection and safety of radiation sources: international basic safety standards. GSR Part 3. International Atomic Energy Agency, Vienna, Austria.

ACKNOWLEDGEMENTS

Sandia National Laboratories is a multimission laboratory managed and operated by National Technology and Engineering Solutions of Sandia, LLC., a wholly owned subsidiary of Honeywell International, Inc., for the U.S. Department of Energy's National Nuclear Security Administration under contract DE-NA-0003525.